Spatial-Temporal Fusion Graph Neural Networks for Traffic Flow Forecasting

Mengzhang Li, Zhanxing Zhu

Peking University, Beijing, China

{mcmong, zhanxing.zhu}@pku.edu.cn

Abstract

Spatial-temporal data forecasting of traffic flow is a challenging task because of complicated spatial dependencies and dynamical trends of temporal pattern between different roads. Existing frameworks typically utilize given spatial adjacency graph and sophisticated mechanisms for modeling spatial and temporal correlations. However, limited representations of given spatial graph structure with incomplete adjacent connections may restrict effective spatial-temporal dependencies learning of those models. Furthermore, existing methods are out at elbows when solving complicated spatial-temporal data: they usually utilize separate modules for spatial and temporal correlations, or they only use independent components capturing localized or global heterogeneous dependencies. To overcome those limitations, our paper proposes a novel Spatial-Temporal Fusion Graph Neural Networks (STFGNN) for traffic flow forecasting. First, a data-driven method of generating "temporal graph" is proposed to compensate several existing correlations that spatial graph may not reflect. SFTGNN could effectively learn hidden spatial-temporal dependencies by a novel fusion operation of various spatial and temporal graphs, treated for different time periods in parallel. Meanwhile, by integrating this fusion graph module and a novel gated convolution module into a unified layer, SFTGNN could handle long sequences by learning more spatial-temporal dependencies with layers stacked. Experimental results on several public traffic datasets demonstrate that our method achieves state-of-the-art performance consistently than other baselines[1].

Introduction

Forecasting task of spatial-temporal data especially traffic data has been widely studied recently because (1) traffic forecasting is one of the most important part of Intelligent Transportation System (ITS) which has great effect on daily life; (2) its data structures is also representative in reality: other location-based data such as wind energy stations, air monitoring stations and cell towers can all be formulated as this spatial-temporal data structure.

Recently, graph modeling on spatial-temporal data has been in the spotlight with the development of graph neural networks. Many works have achieved impressive per-

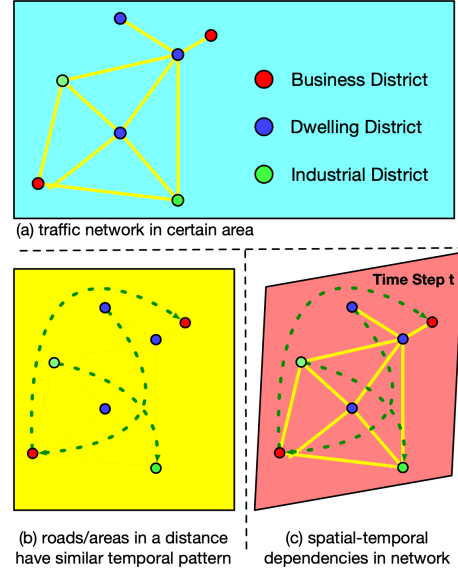[1]Code available at: https://github.com/MengzhangLI/STFGNN

Figure 1: Example of spatial-temporal dependencies in a network. Yellow lines indicate the spatial adjacency in reality. Districts play the same role in traffic network are likely to have similar temporal pattern, which are represented by green dash lines.

formance on prediction accuracy. Although significant improvements have been made in incorporating graph structure into spatial-temporal data forecasting model, these models still face several shortcomings.

The first limitation is being lack of an informative graph construction. Taking Figure 1 for example, those distant nodes may have certain correlations, i.e., they would share similar "temporal pattern". For instance, during rush hours, most roads near the office buildings (from business districts) will encounter traffic jams in the same period. However, most existing models only utilize given spatial adjacency matrix for graph modeling, and *ignore the temporal similarity between nodes when modeling the adjacency matrix*. Some works already made several attempts to improve representation of graph. Mask matrix (Song et al. 2020) and self-adaptive matrix (Wu et al. 2019) are introduced to adjust existed spatial adjacency matrix, but these learnable ma-

trices are both lack of correlations representation ability for complicated spatial-temporal dependencies in graph. Temporal self-attention module (Xu et al. 2020; Wang et al. 2020) of transformers can also extract dynamic spatial-temporal correlations predetermined spatial graph may not reflect. However, it may face overfitting of spatial-temporal dependencies learning due to dynamical change and noisy information in reality data especially in long-range prediction tasks, where autoregressive models can hardly avoid error accumulation.

Besides, current studies of spatial-temporal data forecasting are *ineffective to capture dependencies between local and global correlations*. RNN/LSTM-based models (Li et al. 2017; Zhang et al. 2018) are time-consuming and may suffer gradient vanishing or explosion when capturing long-range sequences. Sequential procedure of transformers (Park et al. 2019; Wang et al. 2020; Xu et al. 2020) may still be time-consuming in inference. CNN-based methods need to stack layers for capturing global correlations of long sequences. STGCN (Yu, Yin, and Zhu 2017) and GraphWaveNet (Wu et al. 2019) may lose local information if dilation rate increases. STSGCN (Song et al. 2020) proposes a novel localized spatial-temporal subgraph that synchronously capture local correlations, which is only designed locally and ignoring global information. When missing data happens, situation is more severe where it would only learn local noise.

To capture both local and global complicated spatial-temporal dependencies, we present a novel CNN-based framework called Spatial-Temporal Fusion Graph Neural Network (STFGNN). Motivated by dynamic time warping (Berndt and Clifford 1994), we propose a novel data-driven method for graph construction: the temporal graph learned based on similarities between time series. Then several graphs could be integrated as a spatial-temporal fusion graph to obtain hidden spatial-temporal dependencies. Moreover, to break the local and global correlation trade-off, gated dilated convolution module is introduced, whose larger dilation rate could capture long-range dependencies. The main contributions of this work are as follows.

- We construct a novel graph by a data-driven method, which preserve hidden spatial-temporal dependencies. This data-driven adjacency matrix is able to extract correlations that given spatial graph may not present. Then, we propose a novel spatial-temporal fusion graph module to capture spatial-temporal dependencies synchronously.

- We propose an effective framework to capture local and global correlations simutaneously, by assembling a Gated dilated CNN module with spatial-temporal fusion graph module in parallel. Long-range spatial-temporal dependencies could also be extracted with layers stacked.

- To make thorough comparisons and test performance in complicated cases, extensive experiments are conducted on eight real-world datasets used in previous works, respectively. The results show our model consistenty outperforms baselines, which strongly proves our proposed model could handle complicated traffic situations in reality with different tarffic characteristics, road numbers and
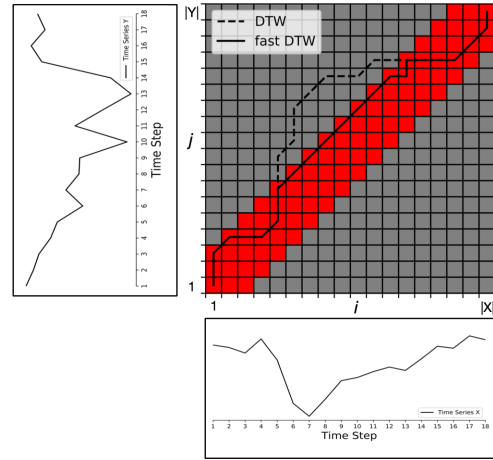

Figure 2: Two time series and their warping path calculated by DTW and fast-DTW algorithm. The red zone is searching zone of fast-DTW defined by "Searching Length" T.

missing value ratios.

Related Works

Graph Convolution Network

Graph convolution network are widely applied in many graph-based tasks such as classification (Kipf and Welling 2016) and clustering (Chiang et al. 2019), which has two types. One is extending convolutions to graphs in spectral domain by finding the corresponding Fourier basis (Bruna et al. 2013). GCN (Kipf and Welling 2016) is representative work and constrcuts typical baselines in many tasks. The other is generalizing spatial neighbours by typical convolution. GAT (Veličković et al. 2017) which introduces attention mechanism into graph filed, and GraphSAGE (Hamilton, Ying, and Leskovec 2017) which generates node embeddings by sampling and aggregating features locally are all typical works.

Spatial-Temporal Forecasting

Spatial-temporal prediction plays an important role in many application areas. To incoporate spatial dependencies more effectively, recent works introduce graph convoluntional network (GCN) to learn the traffic networks. DCRNN (Li et al. 2017) utilizes the bi-directional random walks on the traffic graph to model spatial information and captures temporal dynamics by gated recurrent units (GRU). Transformer models such as (Wang et al. 2020; Park et al. 2019) utilize spatial and temporal attention modules in transformer for spatial-temporal modeling. They would be more effective when training than LSTM but still make predictions step by step due to their auto-regressvie structures. STGCN (Yu, Yin, and Zhu 2017) and GraphWaveNet (Wu et al. 2019) employed graph convolution on spatial domain and 1-D convolution along time axis. They process graph information and time series separately. STSGCN (Song et al. 2020) make attempts to incoporate spatial and temporal blocks altogether

by localized spatial-temporal synchronous graph convolution module regardless of global mutual effect.

Algorithm 1: Temporal Graph Generation
Input: N time series from $\mathcal{V}(|\mathcal{V}| = N)$
1 W Initialization, reset to zero matrix TDL: Temporal Distance Calculation defined in Alg 2
2 **for** $i = 1, 2, \cdots, N$ **do**
3   **for** $j = 1, 2, \cdots, N$ **do**
4      $dist_{i,j} = \text{TDL}(V_i, V_j)$ (Alg. 2)
5   **end**
6   Sort smallest $k(k \leq N)$ element and their index
     $\mathbf{j} = \{j_1, j_2, \cdots, j_k\}$ s.t.
     $dist_{i,j_1} \leq dist_{i,j_2} \leq dist_{i,j_k}$ **if** $\tilde{j} \in \mathbf{j}$ **then**
     $W_{i,\tilde{j}} = W_{\tilde{j},i} = 1$;
7 **end**
8 **return** Weighted Matrix W of Temporal Graph $\mathcal{G}$.

Similarity of Temporal Sequences

The methods for measuring the similarity between time series can be divided into three categories: (1) timestep-based, such as Euclidean distance reflecting point-wise temporal similarity; (2) shape-based, such as Dynamic Time Warping (Berndt and Clifford 1994) according to the trend appearance; (3) change-based, such as Gaussian Mixture Model(GMM) (Povinelli et al. 2004) which reflects similarity of data generation process.

Dynamic Time Warping is a typical algorithm to measure similarity of time series. Given two time series $X = (x_1, x_2, \cdots, x_n)$ and $Y = (y_1, y_2, \cdots, y_m)$, series distance matrix $\boldsymbol{M_{n \times m}}$ could be introduced whose entry is $M_{i,j} = |x_i - y_j|$. Then cost matrix $\boldsymbol{M_c}$ could be defined:

$$M_c(i, j) = M_{i,j} + \min(M_c(i, j-1), M_c(i-1, j), M_c(i, j)) \quad (1)$$

After several iterations of i and j, $dist(X, Y) = M_c(n, m)^{\frac{1}{2}}$ is the final distance between X and Y with the best alignment which can represent the similarity between two time series.

From Eq. (1) we can tell that Dynamic Time Warping is an algorithm based on dynamic programming and its core is solving the warping curve, i.e., matchup of series points x_i and y_j. In other words the "warping path" $\boldsymbol{\Omega}$

$$\Omega = (\omega_1, \omega_2, \cdots, \omega_\lambda), \quad \max(n, m) \leq \lambda \leq n + m$$

is generated through iterations of Eq. (1). Its element $\omega_\lambda = (i, j)$ means matchup of x_i and y_j.

Preliminaries

We can represent the road network as a graph $\mathcal{G} = (V, E, A_{SG})$, where V is a finite set of nodes $|V| = N^2$, corresponding to the observation of N sensors or roads; E is a set of edges and $A_{SG} \in \mathbb{R}^{N \times N}$ is a spatial adjacency

---

[2] In this paper, N represents number of traffic roads/nodes, n represents given length of certain time series. They are totally different.

---

matrix representing the nodes proximity or distance. Denote the observed graph signal $X_{\mathcal{G}}^{(t)} \in \mathbb{R}^{N \times d}$ means it represent the observation of spatial graph information $\mathcal{G}$ at time step t, whose element is observed d traffic features(e.g., the speed, volume) of each sensor. The aim of traffic forecasting is learning a function f from previous T speed observations to predict next T' traffic speed from N correlated sensors on the road network.

$$[\mathbf{X}_{\mathcal{G}}^{(t-T+1)}, \cdots, \mathbf{X}_{\mathcal{G}}^t] \xrightarrow{f} [\mathbf{X}_{\mathcal{G}}^{t+1}, \cdots, \mathbf{X}_{\mathcal{G}}^{t+T'}] \quad (2)$$

Algorithm 2: Temporal Distance Calculation (TDL)
Input: $X = (x_1, \cdots, x_n) \in \mathbb{R}^{n \times d}$,
     $Y = (y_1, \cdots, y_m) \in \mathbb{R}^{m \times d}$, Searching Length T
1 **for** $i = 1, 2, \cdots, n$ **do**
2   **for** $j = \max(0, i - T), \cdots, \min(m, i + T + 1)$ **do**
3      $M_{i,j} = |X_i - Y_j|$;
4   **if** $i = 0, j = 0$ **then** $M_C(i, j) = M_{i,j}^2$;
5   **else if** $i = 0$ **then** $M_C(i, j) = M_{i,j}^2 + M_{i,j-1}$;
6   **else if** $j = 0$ **then** $M_C(i, j) = M_{i,j}^2 + M_{i-1,j}$;
7   **else if** $j = i - T$ **then**
       $M_C(i, j) = M_{i,j}^2 + \min(M_{i-1,j-1}, M_{i-1,j})$;
8   **else if** $j = i + T$ **then**
       $M_C(i, j) = M_{i,j}^2 + \min(M_{i-1,j-1}, M_{i,j-1})$;
9   **else** $M_C(i, j) =$
       $M_{i,j}^2 + \min(M_{i-1,j-1}, M_{i,j-1}, M_{i-1,j})$;
10   **end**
11 **end**
12 **return** $dist(X, Y) = M_C(n, m)^{\frac{1}{2}}$

Spatial-Temporal Fusion Graph Neural Networks

We present the framework of Spatial-Temporal Fusion Graph Neural Network in Figure 3. It consists of (1) an input layer, (2) stacked Spatial-Temporal Fusion Graph Neural Layers and (3) an output layer. The input and output layer are one and two Fully-Connected Layer followed by activation layer such as "ReLU" (Nair and Hinton 2010) respectively. Every Spatial-Temporal Fusion Graph Layer is constructed by several Spatial-Temporal Fusion Graph Neural Modules (STFGN Modules) in parallel and a Gated CNN Module which includes two parallel 1D dilated convolution blocks.

Spatial-Temporal Fusion Graph Construction

The aim of generating temporal graph is to achieve certain graph structure with more accurate dependency and genuine relation than spatial graph. Then, incorporating temporal graph into a novel spatial-temporal fusion graph, which could **make deep learning model lightweight** because this fusion graph already has correlation information of each node with its (1) spatial neighbours, (2) nodes with similar temporal pattern, and (3) own previous or later situation along time axis.

However, generating temporal graph based on similarity of time series by DTW is not easy, it is a typical dynamic programming algorithm with computational complexity $\mathcal{O}(n^2)$. Thus it might be unacceptable for many applications because time series of real world is usually very long. To reduce complexity of DTW, we restrict its "Search Length" T. The searching space of warping path is circumscribed by:

$$\omega_k = (i, j), \quad |i - j| \leq T \tag{3}$$

Consequently, the computational complexity of DTW is reduced from $\mathcal{O}(n^2)$ to $\mathcal{O}(Tn)$ which made its application on large scale spatial-tempral data possible. We name it "fast-DTW".

As shown in Figure 2, given two roads' time series whose length is $|X|$ and $|Y|$, repectively. The distance of those two time series $M_c(|X|, |Y|)$ could be calculated by Eq. (1). The warping path of fast-DTW is restrcited near the diagonal (red zone in Figure 2), consequently the cost of calculating match i and j of the element $\omega_\lambda = (i, j)$ of warping path Ω is not as expensive as DTW algorithm.

The set of α which determines how many smallest numbers are treated in Alg. 1 is tricky and we would analysis it in the section of experiments. Empirically, we keep the sparisity of Temporal Graph A_{TG} almost the same as Spatial Graph A_{SG}.

Figure 3(b) is the example of Spatial-Temporal Fusion Graph. It consists of three kinds $N \times N$ matrix: Spatial Graph A_{SG} which is given by dataset, Temporal Graph A_{TG} generated by Alg. 1, and Temporal Connectivity graph A_{TC} whose element is nonzero iif previous and next time steps is the same node. Given Spatial-Temporal Fusion Graph $A_{STFG} \in \mathbb{R}^{3N \times 3N}$, and taken A_{TG} within a red circle in Figure 3(b) for instance. It denotes the connection between same node from time step: 2 to 3 (current time step $t = 2$). For each node $l \in \{1, 2, \cdots, N\}$, $i = (t+1)*N+l = 3N+l$ and $j = t*N + l = 2N + l$, then $A_{STFG(i,j)} = 1$. To sum up, Temporal Connectivity graph denotes connection of the same node at proximate time steps.

Finally, Spatial-Temporal Fusion Graph $A_{STFG} \in \mathbb{R}^{KN \times KN}$ is generated. Altogether with the sliced input data of each STFGN Module:

$$h^0 = [X_{\mathcal{G}}^{(t)}, \cdots, X_{\mathcal{G}}^{(t+K)}] \in \mathbb{R}^{K \times N \times d \times C} \tag{4}$$

It is sliced iteratively from total input data:

$$X = [X_{\mathcal{G}}^{(t)}, \cdots, X_{\mathcal{G}}^{(t+T)}] \in \mathbb{R}^{T \times N \times d \times C} \tag{5}$$

$X_{\mathcal{G}}^{(t)}$ is high-dimension feature of original data $\mathbf{X}_{\mathcal{G}}^{(t)}$. C is the number of input feature channel from STFGN module, which is also the number of output feature channel from input layer.

Spatial-Temporal Fusion Graph Neural Module

In Spatial-Temporal Fusion Graph Neural Module (STFGN Module), the lightweight deep learning model could extract hidden spatial-temporal dependencies by several simple operations such as matrix multiplication with Spatial-Temporal Fusion Graph A_{STFG}, residual connections and maxpooling.

In this paper, regular spectral filter such as Laplacian in graph convolution is replaced with a more simplified and time-saving operation: matrix multiplication. Each node in network could aggregate spatial dependency from A_{SG}, temporal pattern correlation from A_{TG} and its own proximate correlation long time axis from A_{TC} by several times matrix multiplication with A_{STFG}.

Gating mechanism in LSTM/RNN is also utilized in graph multiplication block. In STFGN Module, gated linear units is used for generalization in graph multiplication by its nonlinar activation. Graph multiplication module is formulated as below:

$$h^{l+1} = (A^* h^l W_1 + b_1) \odot \sigma(A^* h^l W_2 + b_2) \tag{6}$$

where h^l denotes l-th hidden states of certain STFGN module. A^* is shorthand of spatial-temporal fusion graph $A_{STFG} \in \mathbb{R}^{KN \times KN}$, $W_1, W_2 \in \mathbb{R}^{C \times C}$, $b_1, b_2 \in \mathbb{R}^C$ are all model parameters of GLU. $\odot$ means Hadamard product and σ means sigmoid function.

By stacking L graph multiplication blocks, more complicated and non-local spatial-dependencies could be aggregated. Intuitively, the residual connections (He et al. 2016) would also be introduced for each block. MaxPooling would be operated on the concatenation of each hidden state $h^M = MaxPool([h^1, \cdots, h^L]) \in \mathbb{R}^{K \times N \times d \times C}$. Finally this concatenation corresponding to the middle time step would be cropped, saving

$$h^o = h^M \big[\lfloor \frac{K}{2} \rfloor : \lfloor \frac{K}{2} \rfloor + 1, :, :, : \big] \in \mathbb{R}^{1 \times N \times d \times C}$$

Figure 3(b) shows this cropped feature has contained complicated heterogeneity. In each matrix multiplication, A_{SG} in the middle of diagonal (corresponding to cropped location of concatenation) transmit information from spatial neighbour. A_{TC} in its horizontal and vertical direction gives each node its own information along time axis. A_{TG} in corner enhance information from nodes with similar temporal pattern.

Input data would be treated by multiple STFGN Modules independently in parallel, which is time-saving and could capture more complicated correlations. Then concatenation of each STFGN module output would be added with Gated CNN output and becomes input of next STFGN layer. Noted that the size of each STFGN module output is $\mathbb{R}^{(T-K+1) \times N \times d \times C}$, i.e., each STFGN layer would cut input from T to $T - K + 1$ in time dimensions. It means STFGN layers could stack up to $\lfloor \frac{T}{K-1} \rfloor - 1$ layers.

Gated Convolution Module

Although A_{STFG} could extract global spatial-temporal dependencies by integration of A_{TG}, the correlation it contains is more from nodes in a distant (like the example from Figure 1). Long-range spatial-temporal dependencies of the node itself is also important, which is very challenging for many CNN-based works (Yu, Yin, and Zhu 2017; Wu et al. 2019; Song et al. 2020) because inborn structure of CNN can hardly outperform auto-regressive models like transformer(Park et al. 2019; Wang et al. 2020). Different from
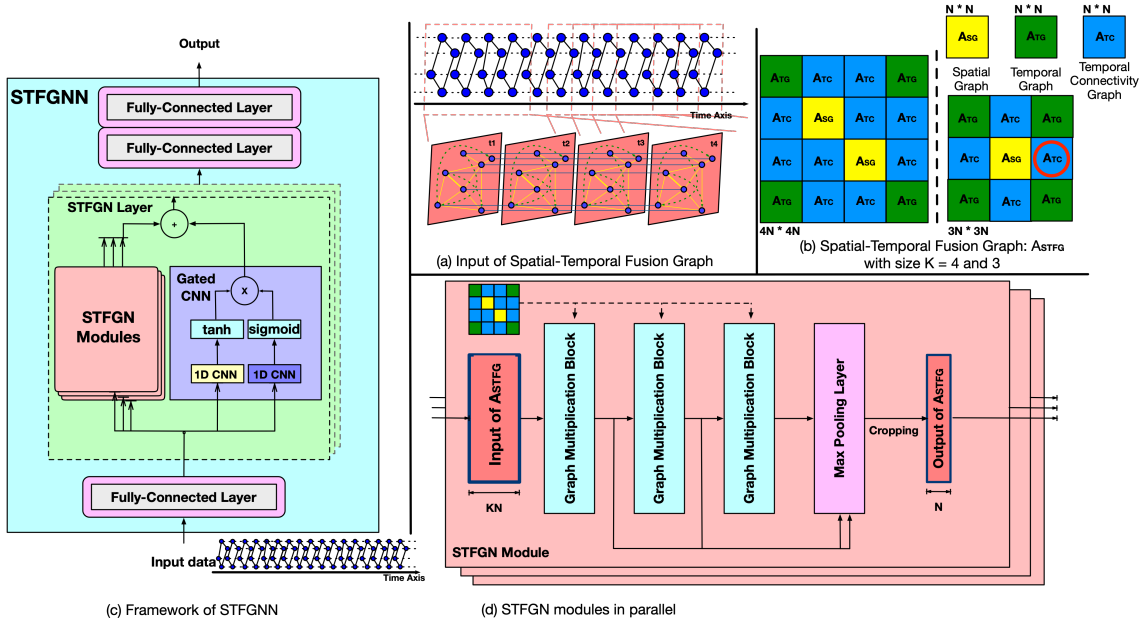
Figure 3: Detailed framework of STFGNN. (a) is the example of input of Spatial-Temporal Fusion Graph, which would be generated iteratively along the time axis. (b) is the example of Spatial-Temporal Fusion Graph, whose size K is 4 and 3, respectively. It consists of three kinds of adjacency matrix $\in N \times N$: spatial graph A_{SG}, temporal graph A_{TG} and temporal connectivity graph A_{TC}. The A_{TC} within a red circle would be taken for instance in the body. (c) is overall structure of STFGNN, its Gated CNN module and STFGNN modules are in parallel. (d) is detailed architecture of the Spatial-Temporal Fusion Graph Modules, each module will be independently trained for input iteratively generated from (a) in parallel as well.

previous work like GraphWaveNet and STGCN, dilated convolution with large dilation rate is introduced in this paper. Given the total input data $X \in \mathbb{R}^{T \times N \times d \times C}$, it takes the form:

$$Y = \phi(\Theta_1 * X + a) \odot \sigma(\Theta_2 * X + b) \qquad (7)$$

Similar with Eq. (6), $\phi(\cdot)$ and $\sigma(\cdot)$ are tanh and sigmoid function, respectively. Θ_1 and Θ_2 are two independent 1D convolution operation with dilation rate = K -1. It could enlarge receptive filed along time axis thus strengthen model performance for extracting sequential dependencies.

Huber loss is chosen as loss function, objective function is shown below:

$$L(\hat{\mathbf{X}}_{\mathcal{G}}^{(t+1):(t+T)}, \Theta) = \frac{\sum_{i=1}^{T} \sum_{j=1}^{N} \sum_{k=1}^{d} h(\hat{\mathbf{X}}_{\mathcal{G}}^{(t+i)}, \mathbf{X}_{\mathcal{G}}^{(t+i)})}{T \times N \times d} \qquad (8)$$

$$h(\hat{Y}, Y) = \begin{cases} \frac{1}{2}(\hat{Y} - Y)^2, & |\hat{Y} - Y| \leq \delta \\ \delta|\hat{Y} - Y| - \frac{1}{2}\delta^2, & |\hat{Y} - Y| > \delta \end{cases}$$

δ is hyperparameter to control sensitivity of squared error loss.

Experiments

Datasets

We verify the performance of STFGNN on eight public traffic network datasets. METR-LA and PEMS-BAY re-

Datasets	#Nodes	#Edges	#TimeSteps	#MissingRatio
METR-LA	207	1515	34272	8.109%
PEMS-BAY	325	2369	52116	0.003%
PeMSD7(M)	228	1132	12672	0
PeMSD7(L)	1026	10150	12672	0
PEMS03	358	547	26208	0.672%
PEMS04	307	340	16992	3.182%
PEMS07	883	866	28224	0.452%
PEMS08	170	295	17856	0.696%

Table 1: Dataset description and statistics.

leased by (Li et al. 2017), PeMSD7 (M) and PeMSD7(L) released by (Yu, Yin, and Zhu 2017) and PEMS03, PEMS04, PEMS07, PEMS08 released by(Song et al. 2020). METR-LA records four months of traffic flow on 207 sensors on the highways of Los Angeles County. PEMS-BAY records six months of traffic speed on 325 sensors in Bay Area. PEMS03, PEMS04, PEMS07 and PEMS08 are constructed from four districts, respectively in California. All these data is collected from the Caltrans Performance Measurement System (PeMS) and aggregated into 5-minutes windows, which means there are 288 points in the traffic flow for one day. The spatial adjacency networks for each dataset is constructed by actual road network based on distance. Z-score normalization is adopted to standardize the data inputs. The detailed information is shown in Table 1.

Datasets	Models	15min			30min			60min		
		MAE	MAPE(%)	RMSE	MAE	MAPE(%)	RMSE	MAE	MAPE(%)	RMSE
METR-LA	ARIMA	3.99	9.60	8.21	5.15	12.70	10.45	6.90	17.40	13.23
	FC-LSTM	3.44	9.60	6.30	3.77	10.90	7.23	4.37	13.20	8.69
	DCRNN	2.77	7.30	5.38	3.15	8.80	6.45	3.60	10.50	7.60
	STGCN	2.88	7.62	5.74	3.47	9.57	7.24	4.59	12.70	9.40
	STSGCN	*3.43*	*9.73*	*6.57*	*3.60*	*10.35*	*6.96*	*3.95*	*11.65*	*7.77*
	GraphWaveNet	2.69	6.90	5.15	3.07	8.37	6.22	3.53	10.01	7.37
	STGRAT	2.60	6.60	5.07	3.01	8.15	6.21	3.49	10.01	7.42
	STGNN	2.62	6.55	4.99	2.98	7.77	5.88	3.49	9.69	6.94
	STFGNN	**2.57±0.01**	**6.51±0.05**	**4.73±0.03**	**2.83±0.00**	**7.46±0.01**	**5.46±0.02**	**3.18±0.01**	**8.81±0.08**	**6.40±0.03**
PEMS-BAY	ARIMA	1.62	3.50	3.30	2.33	5.40	4.76	3.38	8.30	6.50
	FC-LSTM	2.05	4.80	4.19	2.20	5.20	4.55	2.37	5.70	4.96
	DCRNN	1.38	2.90	2.95	1.74	3.90	3.97	2.07	4.90	4.74
	STGCN	1.36	2.90	2.96	1.81	4.17	4.27	2.49	5.79	5.69
	STSGCN	*2.54*	*5.88*	*4.79*	*2.60*	*6.03*	*4.93*	*2.71*	*6.39*	*5.28*
	GraphWaveNet	1.30	2.73	2.74	1.63	3.67	3.70	1.95	4.63	4.52
	STGRAT	1.29	2.67	2.71	1.61	3.63	3.69	1.95	4.64	4.54
	STGNN	1.17	**2.34**	2.43	1.46	3.09	3.27	1.83	4.15	4.20
	STFGNN	**1.16± 0.01**	2.41 ± 0.02	**2.33± 0.02**	**1.39± 0.01**	**3.02± 0.03**	**3.02± 0.02**	**1.66± 0.00**	**3.77± 0.03**	**3.74± 0.03**

Table 2: Performance comparison of STFGNN and baseline models on METR-LA and PEMS-BAY datasets.

Baseline Methods

We compare STFGNN with those following models:

- ARIMA: Auto-Regressive Integrated Moving Average model (Box and Pierce 1970), which is a typical statistical model in time series field.

- FC-LSTM: Long Short-Term Memory Network, which is a recurrent neural network with fully connected LSTM hidden units(Sutskever, Vinyals, and Le 2014).

- DCRNN: Diffusion Convolution Recurrent Neural Network, which integrates graph convolution into a encoder-decoder gated recurrent unit(Li et al. 2017).

- STGCN: spatio-temporal Graph Convolutional Networks, , which integrates graph convolution into a 1D convolution unit(Yu, Yin, and Zhu 2017).

- ASTGCN(r): Attention Based Spatial Temporal Graph Convolutional Networks, which introduces spatial and temporal attention mechanisms into model. Only recent components of modeling periodicity is taken to keep fair comparison(Guo et al. 2019).

- GraphWaveNet: Graph WaveNet is a framework combines adaptive adjacency matrix into graph convolution with 1D dilated convolution(Wu et al. 2019).

- STSGCN: Spatial-Temporal Synchronous Graph Convolutional Networks, which utilizes localized spatial-temporal subgraph module to model localized correlations independently(Song et al. 2020).

- STGRAT: Spatio-Temporal Graph Attention Network, which utilizes adapted spatial and temporal self-attention module in transformer model(Park et al. 2019).

- STGNN: Spatial Temporal Graph Neural Network, which is also a complicated transformer model with a learnable positional attention mechanism and a sequential component(Wang et al. 2020).

Experiment Settings

To make fair comparison with previous baselines, we split the data totally the same: with ratio 7 : 1 : 2 at METR-LA, PEMS-BAY, PeMSD7(M) and PeMSD7(L), and 6 : 2 : 2 at PEMS03, PEMS04, PEMS07, PEMS08 into training sets, validation sets and test sets. One hour 12 continuous time steps historical data is used to predict next hour's 12 continuous time steps data. STFGNN is evaluated more than 10 times in each public dataset.

Experiments are conducted under the environment with one Intel(R) Xeon(R) Gold 6240 CPU @ 2.60GHz and NVIDIA TESLA V100 GPU 16GB card. The temporal graph A_{TG} generated by fast-DTW in Alg. 1 costs less than 30 minutes in most public datasets. The Searching Length "T" in "fast-DTW" algorithm is 12, which is the largest prediction time steps in our traffic forecasting task. The sparsity of A_{TG} is 0.01. The model contains 3 STFGNLs, where each contains 8 independent STFGNMs and 1 gated convolution module with dilation rate 3 because the size K of spatial-temporal fusion graph we use is 4. Elements of all three kinds graph are booled to 0 or 1 for the sake of simplification. Filters in each convolution are all 64. We train our model using Adam optimizer with learning rate 0.001. The threshold parameter of loss function δ is 1, the batch size is 32 and the training epoch is 200.

Experiment Results and Analysis

Table 2, Table 3 and Table 4 show the through comparison between different models. Results show our STFGNN outperforms baseline models consistently and overwhelmingly on every dataset except only one metric of short-range MAPE in PEMS-BAY dataset, which is slighly larger than STGNN.

Results on METR-LA and PEMS-BAY

Due to relatively less node numbers (207 and 325) and more smooth time series (metrics of them are much smaller than counterparts of four PEMS datasets), METR-LA and

Datasets	Metric	FC-LSTM	DCRNN	STGCN	ASTGCN (r)	Graph WaveNet	STSGCN	STFGNN
PEMS 03	MAE	21.33	18.18	17.49	17.69	*19.85*	17.48	**16.77± 0.09**
	MAPE(%)	23.33	18.91	17.15	19.40	*19.31*	16.78	**16.30± 0.09**
	RMSE	35.11	30.31	30.12	29.66	*32.94*	29.21	**28.34± 0.46**
PEMS 04	MAE	27.14	24.70	22.70	22.93	*25.45*	21.19	**19.83± 0.06**
	MAPE(%)	18.20	17.12	14.59	16.56	*17.29*	13.90	**13.02± 0.05**
	RMSE	41.59	38.12	35.55	35.22	*39.70*	33.65	**31.88± 0.14**
PEMS 07	MAE	29.98	25.30	25.38	28.05	*26.85*	24.26	**22.07± 0.11**
	MAPE(%)	13.20	11.66	11.08	13.92	*12.12*	10.21	**9.21± 0.07**
	RMSE	45.94	38.58	38.78	42.57	*42.78*	39.03	**35.80± 0.18**
PEMS 08	MAE	22.20	17.86	18.02	18.61	*19.13*	17.13	**16.64± 0.09**
	MAPE(%)	14.20	11.45	11.40	13.08	*12.68*	10.96	**10.60± 0.06**
	RMSE	34.06	27.83	27.83	28.16	*31.05*	26.80	**26.22± 0.15**

Table 3: Performance comparison of STFGNN and baseline models on PEMS03, PEMS04, PEMS07 and PEMS08 datasets.

	T	Metric	FC-LSTM	DCRNN	STGCN	GraphWaveNet	STSGCN	STFGNN
PeMSD7(M)	15min	MAE	3.57	2.25	2.24	2.14	1.99	**1.83± 0.01**
		MAPE%	8.60	5.30	5.20	4.93	4.62	**4.27± 0.04**
		RMSE	6.20	4.04	4.07	4.01	3.59	**3.34± 0.02**
	30min	MAE	3.92	2.98	3.02	2.80	2.43	**2.23± 0.01**
		MAPE%	9.55	7.39	7.27	6.89	5.83	**5.39± 0.05**
		RMSE	7.03	5.58	5.70	5.48	4.63	**4.30± 0.02**
	60min	MAE	4.16	3.83	4.01	3.19	3.04	**2.71± 0.01**
		MAPE%	10.10	9.85	9.77	8.04	7.62	**6.76± 0.04**
		RMSE	7.51	7.19	7.55	6.25	6.01	**5.39± 0.03**
PeMSD7(L)	15min	MAE	4.36	2.36	2.37	2.25	2.87	**2.18± 0.25**
		MAPE%	11.10	5.51	5.56	5.22	7.00	**5.20± 0.75**
		RMSE	7.68	4.45	4.32	4.23	5.19	**3.94± 0.41**
	30min	MAE	4.51	3.24	3.27	2.93	3.16	**2.56± 0.20**
		MAPE%	11.41	8.18	7.98	7.27	7.84	**6.27± 0.58**
		RMSE	7.94	6.31	6.21	5.72	5.86	**4.84± 0.26**
	60min	MAE	4.66	4.34	4.35	3.60	3.62	**3.04± 0.19**
		MAPE%	11.69	11.91	11.17	9.45	9.24	**7.71± 0.51**
		RMSE	8.20	8.33	8.27	7.05	6.89	**5.91± 0.18**

Table 4: Performance comparison of STFGNN and baseline models on PeMSD7(M) and PeMSD7(L) datasets.

Dataset	Model Elements	MAE	MAPE%	RMSE
PEMS04	STSGCN	<u>21.19</u>	<u>13.90</u>	<u>33.65</u>
	$[ST_3, T_{sp5}]$	20.74	13.77	33.44
	$[ST_3, T_{sp1}]$	20.09	13.24	32.44
	$[ST_4, T_{sp1}]$	19.92	13.03	31.93
	$[T_4, T_{sp1}, \Theta]$	20.02	13.17	31.98
	$[T_4, T_{sp5}, \Theta]$	19.91	13.11	32.19
	$[ST_4, T_{sp1}, \Theta]$	**19.83**	**13.02**	**31.88**
PEMS08	STSGCN	17.13	10.96	26.80
	$[ST_3, T_{sp5}]$	<u>19.47</u>	<u>12.27</u>	<u>29.59</u>
	$[ST_3, T_{sp1}]$	16.84	10.80	26.58
	$[ST_4, T_{sp1}]$	16.70	10.63	26.24
	$[T_4, T_{sp1}, \Theta]$	18.23	11.52	29.05
	$[T_4, T_{sp5}, \Theta]$	**16.02**	**10.07**	**25.39**
	$[ST_4, T_{sp1}, \Theta]$	16.64	10.60	26.22

Table 5: Ablation experiments on different configurations of modules. ST_4 means A_{STFG} with size k = 4. T_4 means A_{SG} is all replaced to A_{TG} in A_{STFG}. T_{sp5}, T_{sp1} means nonzero ratio of A_{TG} is about 5% and 1%, respectively. Θ represents whether gated convolution module is added into each STFGN layer. The default STFGNN configuration we use in this paper is $[ST_4, T_{sp1}, \Theta]$.

PEMS-BAY are widely used for performance evaluation. Table 2 shows models based on transformers and LSTM/RNN usually outperform others. Transformer models are good at short-range prediction because of good learning ability of their complicated network architectures. But the gap of each metric between STFGNN and transformer models becomes larger when range increases, because error accumulation caused by reality data noise is inevitable for all auto-regressive models.

Modules of STSGCN only extract local spatial-temporal dependencies, and their modules only use multiplication operation (Fully-connected network and adjacency matrix multiplication operation). Thus frequent missing values would disturb its local learning module and smooth time series would magnify its limited representation ability.

Results on PEMS datasets

Followed by metrics previous baseline(Song et al. 2020) takes, Table 3 compares the performance of STFGNN and other models for 60 minutes ahead prediction on PEMS03, PEMS04, PEMS07 and PEMS08 datasets.

All these four datasets are not particularly smooth, the relatively poor performance of GraphWaveNet reveals its struggle because it can not stack its spatial-temporal layers and enlarge receptive fields of 1D CNN concurrently.

Results on PeMSD7 datasets

Although the scale of PeMSD7(L) dataset (1026 nodes) might be challenging for some transformer and LSTM/RNN, no missing value and relatively smooth characteristics are friendly for deep learning models. The consistently best result of STFGNN on PeMSD7(M) and PeMSD7(L) proves its basically good representation ability.

Ablation Experiments

To verify effectiveness of different parts in STFGNN, we conduct ablation experiments on PEMS04 and PEMS08. Table 5 shows metric of MAE, MAPE and RMSE. The "Model Element" represents each configuration. Some conclusions could be drawn:

- For ingredient of A_{STFG}, larger A_{STFG} means more complicated heterogeneity in spatial-temporal dependencies could be extracted regradless of less stacking layers.

- For sparsity of A_{TG}, it is an important hyperparameter, which determines performance of STFGNN. Empirically, it was set based on sparsity of prior spatial graph. We also demonstrate, with proper sparsity of A_{TG}, spatial information free traffic forecasting model is possible, which has promising application value if A_{SG} is unavailable.

- For Gated Convolution Module, it could remedy long-range learning ability of STFGN Modules which could improve performance of STSGNN.

Conclusion

In this paper, we present a novel framework for spatial-temporal traffic data forecasting. Our model could capture hidden spatial-dependencies effectively by a novel data-driven graph and its further fusion with given spatial graph. By integration with STFGN module and a novel Gated CNN module which enlarges receptive filed on temporal sequences and stacking it, STFGNN could learn localized spatial-temporal heterogeneity and global spatial-temporal homogeneity simultaneously. Detailed experiments and analysis reveal advantages and defects of pre-

vious models, which in turn demonstrate STFGNN consistent great performance.

Acknowledgements

References

Berndt, D. J.; and Clifford, J. 1994. Using dynamic time warping to find patterns in time series. In *KDD workshop*, volume 10, 359–370. Seattle, WA, USA:.

Box, G. E.; and Pierce, D. A. 1970. Distribution of residual autocorrelations in autoregressive-integrated moving average time series models. *Journal of the American statistical Association* 65(332): 1509–1526.

Bruna, J.; Zaremba, W.; Szlam, A.; and LeCun, Y. 2013. Spectral networks and locally connected networks on graphs. *arXiv preprint arXiv:1312.6203* .

Chiang, W.-L.; Liu, X.; Si, S.; Li, Y.; Bengio, S.; and Hsieh, C.-J. 2019. Cluster-GCN: An efficient algorithm for training deep and large graph convolutional networks. In *Proceedings of the 25th ACM SIGKDD International Conference on Knowledge Discovery & Data Mining*, 257–266.

Guo, S.; Lin, Y.; Feng, N.; Song, C.; and Wan, H. 2019. Attention based spatial-temporal graph convolutional networks for traffic flow forecasting. In *Proceedings of the AAAI Conference on Artificial Intelligence*, volume 33, 922–929.

Hamilton, W.; Ying, Z.; and Leskovec, J. 2017. Inductive representation learning on large graphs. In *Advances in neural information processing systems*, 1024–1034.

He, K.; Zhang, X.; Ren, S.; and Sun, J. 2016. Deep residual learning for image recognition. In *Proceedings of the IEEE conference on computer vision and pattern recognition*, 770–778.

Kipf, T. N.; and Welling, M. 2016. Semi-supervised classification with graph convolutional networks. *arXiv preprint arXiv:1609.02907* .

Li, Y.; Yu, R.; Shahabi, C.; and Liu, Y. 2017. Diffusion convolutional recurrent neural network: Data-driven traffic forecasting. *arXiv preprint arXiv:1707.01926* .

Nair, V.; and Hinton, G. E. 2010. Rectified linear units improve restricted boltzmann machines. In *ICML*.

Park, C.; Lee, C.; Bahng, H.; Kim, K.; Jin, S.; Ko, S.; Choo, J.; et al. 2019. Stgrat: A spatio-temporal graph attention network for traffic forecasting. *arXiv preprint arXiv:1911.13181* .

Povinelli, R. J.; Johnson, M. T.; Lindgren, A. C.; and Ye, J. 2004. Time series classification using Gaussian mixture models of reconstructed phase spaces. *IEEE Transactions on Knowledge and Data Engineering* 16(6): 779–783.

Song, C.; Lin, Y.; Guo, S.; and Wan, H. 2020. Spatial-Temporal Synchronous Graph Convolutional Networks: A New Framework for Spatial-Temporal Network Data Forecasting. In *Proceedings of the AAAI Conference on Artificial Intelligence*, volume 34, 914–921.

Sutskever, I.; Vinyals, O.; and Le, Q. V. 2014. Sequence to sequence learning with neural networks. In *Advances in neural information processing systems*, 3104–3112.

Veličković, P.; Cucurull, G.; Casanova, A.; Romero, A.; Lio, P.; and Bengio, Y. 2017. Graph attention networks. *arXiv preprint arXiv:1710.10903* .

Wang, X.; Ma, Y.; Wang, Y.; Jin, W.; Wang, X.; Tang, J.; Jia, C.; and Yu, J. 2020. Traffic Flow Prediction via Spatial Temporal Graph Neural Network. In *Proceedings of The Web Conference 2020*, 1082–1092.

Wu, Z.; Pan, S.; Long, G.; Jiang, J.; and Zhang, C. 2019. Graph wavenet for deep spatial-temporal graph modeling. *arXiv preprint arXiv:1906.00121* .

Xu, M.; Dai, W.; Liu, C.; Gao, X.; Lin, W.; Qi, G.-J.; and Xiong, H. 2020. Spatial-Temporal Transformer Networks for Traffic Flow Forecasting. *arXiv preprint arXiv:2001.02908* .

Yu, B.; Yin, H.; and Zhu, Z. 2017. Spatio-temporal graph convolutional networks: A deep learning framework for traffic forecasting. *arXiv preprint arXiv:1709.04875* .

Zhang, J.; Shi, X.; Xie, J.; Ma, H.; King, I.; and Yeung, D.-Y. 2018. Gaan: Gated attention networks for learning on large and spatiotemporal graphs. *arXiv preprint arXiv:1803.07294* .